JVST A
Journal of Vacuum Science & Technology A

Practical guide for x-ray photoelectron spectroscopy: Applications to the study of catalysts

Cite as: J. Vac. Sci. Technol. A **38**, 033204 (2020); https://doi.org/10.1116/1.5140747
Submitted: 30 November 2019 . Accepted: 02 March 2020 . Published Online: 18 March 2020

Philip R. Davies, and David J. Morgan

JVST A
Journal of Vacuum Science & Technology A

ARTICLE

avs.scitation.org/journal/jva

Practical guide for x-ray photoelectron spectroscopy: Applications to the study of catalysts

Cite as: J. Vac. Sci. Technol. A 38, 033204 (2020); doi: 10.1116/1.5140747
Submitted: 30 November 2019 · Accepted: 2 March 2020 ·
Published Online: 18 March 2020

Philip R. Davies[1,2] and David J. Morgan[1,2,a)]

AFFILIATIONS

[1]Cardiff Catalysis Institute, School of Chemistry, Cardiff University, Park Place, Cardiff CF10 3AT, United Kingdom
[2]HarwellXPS—EPSRC National Facility for X-Ray Photoelectron Spectroscopy, Research Complex at Harwell (RCaH), Didcot OX11 0FE, United Kingdom

Note: This paper is part of the Special Topic Collection on Reproducibility Challenges and Solutions.
a)Electronic mail: MorganDJ3@Cardiff.ac.uk

ABSTRACT

X-ray photoelectron spectroscopy (XPS) has become a standard tool for the study of catalytic materials over the last two decades, and with the increasing popularity of turnkey XPS systems, the analysis of these types of materials is open to an even wider audience. However, increased accessibility leads to an increase in the number of new or inexperienced practitioners, leading to erroneous data collection and interpretation. Over many years of working on a wide range of catalytic materials, the authors have developed procedures for the planning and execution of XPS analysis and subsequent data analysis, and this guide has been produced to help users of all levels of expertise to question their approach toward analysis and get the most out of the technique and avoiding some common pitfalls.

I. INTRODUCTION

Heterogeneous catalysis is concerned with the reaction of molecules at active sites located within the surface region of a catalytic material. The reaction itself proceeds via a series of steps including adsorption, surface diffusion, chemical reaction/rearrangement of adsorbed intermediates, and, finally, desorption of products.[1–3] To aid the development of such catalytic systems, modification of the surface chemical, electronic, and structural properties is of extreme importance, and with their inherent surface sensitivity and chemical specificity,[4,5] x-ray photoelectron spectroscopy (XPS) and x-ray excited Auger electron spectroscopy (XAES) have become powerful tools in the armory of the catalytic scientist.[4,6–12]

Catalytic materials present some distinct challenges when it comes to surface analysis: they are often high surface area powders; usually, insulating and the loading of the nanoparticulate active component can be very low (0.5 wt. % or lower). XPS requires ultrahigh vacuum (UHV), while most heterogeneous catalytic reactions take place at high pressures and temperatures; therefore, catalytic materials are typically studied under conditions significantly different from that in which they would normally operate.[2,3] Taking the simple example of a hydrated precursor, insertion into a vacuum environment will lead to dehydration; therefore, the spectra obtained would be of a dehydrated material.[13,14] Nevertheless, analysis under vacuum can yield insightful information into the activity (or lack thereof) and speciation of a catalyst provided the analyst keeps in mind both the opportunities and limitations offered by the technique. Should the analyst require knowledge of samples, which will not be adversely affected by vacuum, they may consider the use of near-ambient pressure XPS or similar.

As part of the series of practical guides for analysis,[15] herein, we discuss some of the advantages XPS can offer to analyze catalytic materials and highlight some of the common pitfalls that may be experienced during the preparation, acquisition, and interpretation of samples and data that we have experienced over many years of working within the catalytic community, and although this article may be focused on catalysis, much of the content herein is transferrable to the analysis of many other materials.

II. SAMPLE PREPARATION AND HISTORY

Successful acquisition of high-quality photoemission requires significant thought toward a number of operating parameters, more of which are introduced in this paper and also referenced in the ISO 10810 standard; however, at the initial level, quality data begin with correct sample preparation. Industrial catalysts are typically in

the form of pellets, extrudates, or monoliths, while within an academic research environment, most catalytic materials presented for analysis are powders generally comprising metallic nanoparticles dispersed on a suitable support material such as carbon or a metal oxide. Immobilization of these powders is paramount, with poorly mounted samples potentially contaminating other samples, something especially true where large sample platens allow for the insertion of multiple sample types.

At this stage, it is worth noting that each of these sample types may have its own analysis requirements. For example, the homogeneity of a powdered catalyst may be assessed by running multiple aliquots from the batch, while an industrial catalyst may require multipoint analysis for statistical relevance to understand the active phase and its dispersion. Additionally, catalysts in either of these instances could consist of a core-shell morphology, which requires a more detailed analysis of the photoelectron signal. We introduce these points in Secs. V D.

A. Sample mounting and preparation

There are universally accepted methods of sample preparation, details of which are documented in ISO 18116 (ASTM E1078) and ISO 18117 (ASTM E1829) standards. Many of these are applicable to the surface analysis of catalysts; however, each method has potential drawbacks as introduced in Table I.

As already mentioned, catalysts can come in many shapes and sizes, and without considered preparation of the sample, XPS analysis can be difficult or give meaningless data. For example, spheres, pellets, and cylindrical extrudates may have their outer surface readily analyzed, while catalysts presented as monoliths, miniliths, hollow extrudates, and rings typically require exposure of the inner channels where the catalytic active species are located. While such samples can potentially be ground into a powder, the volume of the support material compared to the active species can potentially lead to significant dilution of the active species and hence a low signal.

A common requirement with the analysis of catalytic materials is an *in situ* treatment, such as by heating (to desorb weakly held contaminants or to initiate a material transformation) or by subjecting them to a reactive gas flow within the spectrometer, often in a linked "catalysis cell." Such requirements would dictate the method of sample mounting and, with reference to Table I, would preclude options (1) and (5) with options (3) or (4) considered more suitable.

Materials, such as those with significant porosity, may require prolonged periods of outgassing, and such samples should be mounted and analyzed individually where possible to negate potential cross-contamination; this is especially true for materials, which potentially sublime under vacuum (e.g., some halogenated materials[16]), although such materials may be analyzed using a cooled sample stage.[17]

B. Sample history

Sample history is commonly overlooked but is a significant factor that can inform the view of the analyst to the analysis requirements or to the processable data in front of them. This history should include sample preparation and treatment (e.g., a calcination or reduction sequence) and the handling and storage of samples prior to analysis. Documenting the color of a sample prior and post analysis, such as that shown in Fig. 1, is recommended as materials may discolor, indicating an analysis induced change, which could be pertinent to data interpretation or refinement of analysis protocols.

Sample history should also include the medium in which samples were mounted, e.g., an inert atmosphere such as a glove box, or within the laboratory environment itself. Figure 2 shows an example of an iron-based Fischer–Tropsch catalyst, which has undergone a partial reaction under synthesis gas at ~250 °C and removed, under an argon atmosphere, for XPS analysis. In Fig. 2, the lower Fe(2p) spectrum if of the sample which was mounted in the laboratory without any protective atmosphere; the time for mounting and insertion into the spectrometer was under 5 min, while the upper spectrum shows the spectrum of the same sample prepared in a glove bag purged with argon for 30 min prior to preparing. It is evident from these two spectra alone that preparation in the inert atmosphere of the glove bag minimizes re-oxidation of the metallic iron compared to that of the laboratory.

The spectra in Fig. 2 clearly show that mounting in the inert atmosphere of a glove bag is more indicative of the true extent for iron reduction, which may undoubtedly be improved further where dedicated glove boxes with oxygen and moisture monitoring can be

TABLE I. Common mounting methods for catalytic samples arranged in the order of authors' typical preference of mounting.

Mounting method	Benefits	Potential drawbacks
(1) Pressed into tape	• Simple • Cheap	• Possible silicone/organic contamination • Cannot pretreat/heat samples
(2) Mounted into a recess	• Simple • Minimizes the chance of contamination	• Potential for sample loss (via turbulent flow or vibrations)
(3) Drop casting onto Si	• Smooth, thin layer • Negligible charging • *In situ* treatment possible	• Organic solvent residue • Possibility of surface modification • Possible substrate peaks in spectra
(4) Pelletized	• Pretreatment possible • High signal intensity	• Preparation could lead to contamination from a pellet press • Not all samples good for pressing
(5) Pressed into indium foil	• Excellent charge neutralization • Considered truly UHV compatible	• Costly (Al or Cu can be used as cheaper alternatives) • Potential for In signals in spectra

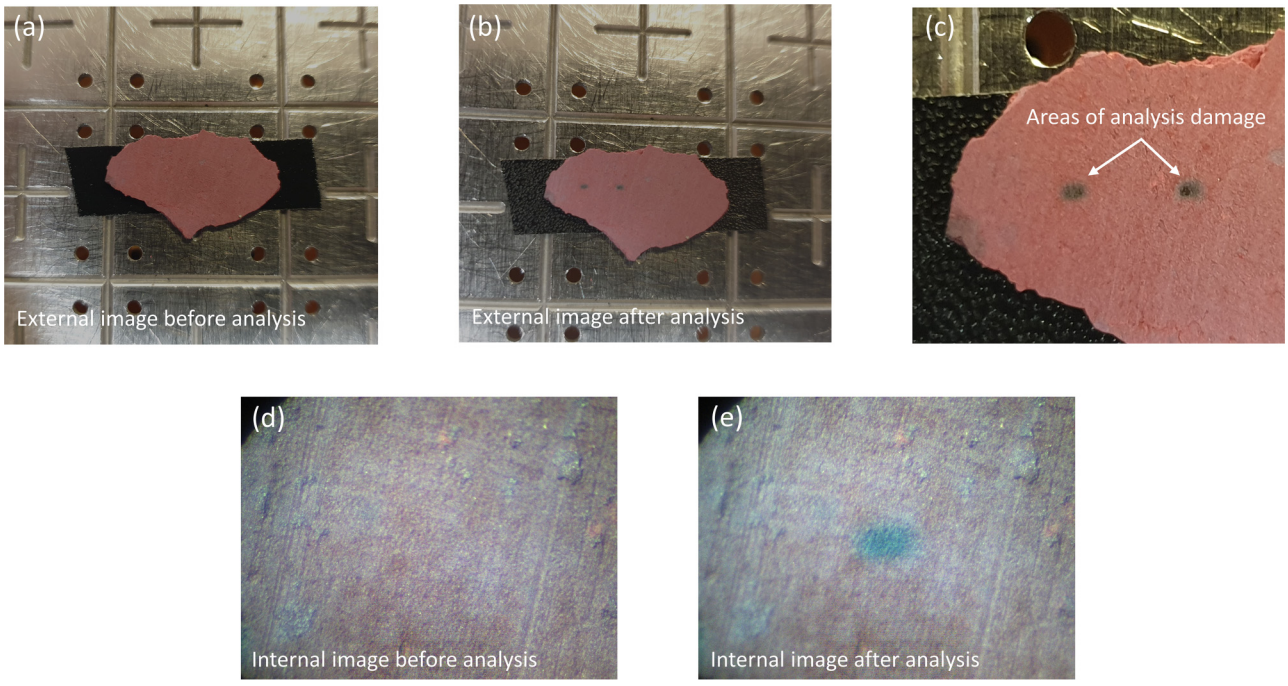

FIG. 1. Example of a color change, which may be documented in the sample history. This example is of a CrO_3 flake, where (a) and (b) show the externally taken photographs of the samples before and after analysis, while (c) shows an enlarged area of the two analysis points. Images (d) and (e) show the same sample taken with the internal optical camera of the spectrometer before and after analysis.

used. Nevertheless, should such a glove box not be directly attached to the spectrometer, a weak link of transportation to the spectrometer still exists, and therefore, dedicated inert-gas or vacuum transfer devices should be used.

III. EXPERIMENTAL PLANNING

The analyst may have an idea as to what elements are present and to be analyzed; however, typical questions such as those presented in Table II should always be asked when planning and setting out the experimental flow within the acquisition software.

Sample modification during XPS analysis is well known in the analysis of polymers.[20,21] For heterogeneous catalysts, analysis induced reduction is often observed with samples containing high valence states of Au,[22,23] Pd,[24] Re,[25] and Cu,[26] among others.[27] Excellent reviews of this topic have been given by Baer *et al.*[28] and Thomas[29] together with a discussion on the mechanism of reduction. Although considered to be primarily caused by secondary electron emission, it has recently been shown that without fine-tuning the operating modes of a dual charge compensation source, there may be a significant reduction in at least two important classes of catalytic materials, specifically high-valence transition metal oxides and metal-organic frameworks, an example of the improvement, which can be gained, is shown in Fig. 3 for CrO_3, while Fig. 1 shows the physical changes, which occur in this particular sample.[30] For information on optimization of charge compensation systems, a future practical guide will focus on this, but analysts are encouraged to read the ISO 19318 (ASTM E1523) standard on charge control and reporting.

Such phenomena can potentially be mitigated by the addition of rapid multipoint analysis spectra, reduced x-ray power, modified neutralizer settings, or sample precooling, and all form part of the informed experimental approach to capture the "true" surface chemistry. Table II attempts to summarize the questions an experimentalist should ask before undertaking an analysis of a catalytic sample. It is, therefore, prudent to critically review acquired data with respect to unexpected chemical states.

As highlighted in the introduction, many supported catalysts have low loadings of the active nanoparticulate phase, which depending on particle size and dispersion will have an influence on the photoelectron signal.[31–33] Identification of the supported phase, therefore, may require prolonged acquisition times to improve signal-to-noise levels (which has a square root dependence for improvement) and may also be accompanied by a modest increase in the pass energy employed for all regions (e.g., 40 eV instead of 20 eV) to collect more photoelectron signals but at the expense of a slight loss in resolution.

IV. BINDING ENERGIES AND SPECTRAL CALIBRATION—IS CARBON THE IDEAL CHOICE?

The reporting of binding energies for conducting materials is straightforward, providing the user has a well characterized energy scale;[34] however, catalytic materials are typically insulating.

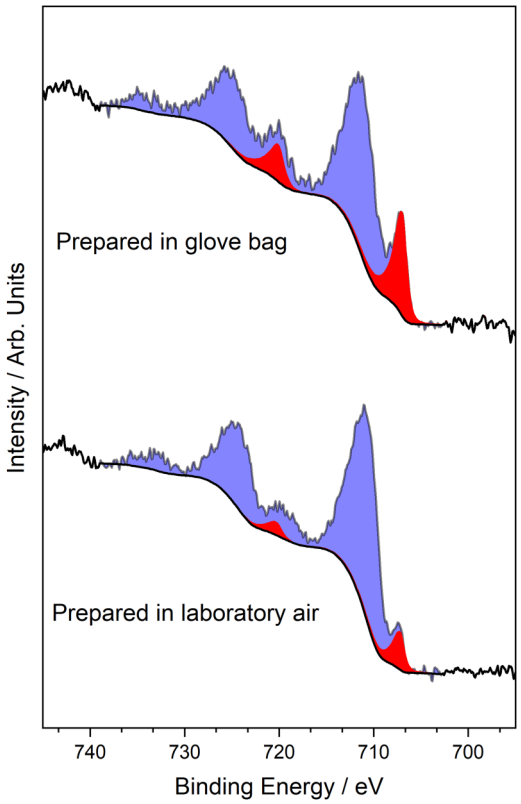

FIG. 2. Fe(2p) spectra for an Fe based Fischer–Tropsch catalysts, illustrating the difference between the same catalyst mounted in laboratory air and the same catalyst mounted in a glove bag above the load-lock of the spectrometer. The relative concentration of metallic Fe (lower binding energy sharp peak, colored red online), with respect to the oxide (broader higher binding energy species, colored blue online), is ~8% and 20% in the lower and upper spectra, respectively. Note, for simplicity, Fe(III) and Fe(II) oxides have been treated as a single oxide phase in the figure.

The choice of a well-defined and stable reference point is, therefore, a paramount concern to the analyst as significant shifts in the binding energy of the supported nanoparticles can occur depending on, for example, support composition, alloy formation, the interaction with the support and Strong Metal Support Interaction (SMSI) effects, or nanoparticle size and shape.[10,35–40]

It is commonplace to calibrate to the C(1s) peak of adventitious carbon, typically assigned a value between 284.5 eV (sp2 carbon) and 285 eV (sp^3 carbon),[41] although it has long been established that this method is far from ideal[40,42–45] and may also be complicated by the presence of overlapping species such as Ru.[46] Recently, Jacquemin *et al.*[47] and Greczynski and Hultman[48,49] have revisited carbon charge referencing, concluding that while such calibration may be suitable for comparison of similar samples, carbon referencing will always have a significant uncertainty, largely due to differences in the underlying inorganic material. Such an example of this is shown in Fig. 4, where the spectra show the Mg(2s)/Au(4f) and C(1s) core levels for the same Au/MgO catalyst taken before and after calcination.

The spectra are presented that are calibrated to the mean literature value for Mg(2s) for MgO taken from the National Institute of Standards and Technology (NIST) database.[50] It is evident from the overlay spectra that the C(1s) for the calcined catalyst is shifted downward in binding energy by 0.6 eV if calibrated to the Mg(2s) support peak, which may be assumed not to change. However, calcination will typically change the nature of the support, specifically altering the acid-base properties, which will have an influence on the electronic environment of species on the surface; hence, further elucidation of any change in the support (see, for example, Sec. V B) may require investigation.

While the panacea of a reliable, static calibration source for insulating samples is still far from sight, the ubiquitous nature of adventitious carbon means that it remains a suitable candidate as an internal reference. However, other peaks such as O(1s) for metal oxides obtained from thin films,[51] or a core level not strongly perturbed by a change in the oxidation state such as $Zn(2p_{3/2})$,[9] Si(2p) in SiO_2,[52] or the high binding energy Ce^{4+} peak (so-called U^{iii}, arising from a Ce^{4+} $3d^94f^0O2p$ (Ref. 6) final state[53,54]) for CeO_2[55,56] may potentially be used as suitable alternatives if the analyst is unsure on the reliability of the C(1s) value. Whatever is chosen as a reference, provided there is no significant change in substrate composition and the calibration value is reported, the data obtained may be compared with similarly well-defined data in the open literature and in databases such as NIST (Ref. 50) or Surface Science Spectra.[57]

V. SPECTRAL INTERPRETATION

Photoelectron spectra contain a wealth of qualitative and quantitative information, but in some circumstances, they can be extremely complex with the spectra of lanthanides as prime examples.[58] Such complexity poses real challenges to even the most experienced analysts, and one must always be on guard against commonly encountered errors such as incorrectly attributing peak asymmetry, satellite structure, multiplet splitting, or screened photoemission peaks to nonstoichiometric or high oxidation states (see, for example, Refs. 59–66). An excellent paper on the use and misuse of curve fitting is given by Sherwood,[67] and we highlight some of the points raised in that paper in Secs. V A–V E.

A. Spectral line shapes

Extraction of chemical states (e.g., Pd^0 versus Pd^{2+}) from photoelectron spectra often requires spectral fitting, and care must be taken to ensure that the shape of the fitting function is well suited to the peak concerned; the shape of the photoelectron peak from one oxidation state cannot be assumed to be the same as that of another.

In part, such mistakes stem from the application of simple Gaussian or mixed Gaussian–Lorentzian functions to photoelectron spectroscopy data to facilitate chemical state identification. While these line shapes may adequately describe polymers or the simplest metal oxides, this is not always the case for metals, especially without an appreciation of the relevant spin–orbit splitting or the area ratio of such peaks.

Metals have a distribution of unfilled electron levels above the Fermi level that are available for shake-up following photoemission; thus, instead of observing discrete satellite features on the high binding energy side, the peak exhibits an extended tail. For a metal

TABLE II. Typical questions the analyst should consider when preparing catalytic materials for analysis. Many of the points are discussed in the text.

Question	Possible action
Do I know all elements present?	• Record survey spectra and assess elements to be recorded • Potentially record survey spectra on the mounted replicate sample in the case of x-ray induced damage?
Am I looking solely for the evidence of a catalytic poison such as S or Cl?	• Record high pass energy survey spectra only
Are reducible elements present?	• Record analysis sensitive elements first and again at the end • Possibly minimize the number of scans or use summation of multipoint analysis for better signal to noise • Modify x-ray power or charge neutralizer settings
Can I be confident of chemical state determination from core levels alone?	• Record Auger lines
Do any peaks overlap?	• Record core levels, which exhibit multiplet splitting • Additionally, record other core levels with sufficient photoelectron intensity. Possibly, use different excitation sources
Is *in situ* treatment required?	• Select the correct method of mounting
Will exposure to the atmosphere modify the sample?	• Consider the use of inert transfer and/or glovebox
Do I need to record the valence region?	• E.g., low concentrations of Ti^{3+} defects and Sn oxidation states may be more readily distinguished by this method (Refs. 18 and 19)
Do I have volatile species I need to analyze?	• Precool entry and analysis stages
Is the concentration of supported nanoparticles low?	• Increase the number of scans for the element in question • Consider running the acquisition at higher pass energy (e.g., 40 eV instead of 20 eV)

with a high density of states at the Fermi level such as platinum, this effect is greatly pronounced, resulting in a high degree of peak asymmetry.[68,69] The effect is illustrated in Fig. 5, which shows the extended tail to the high binding energy side of the Pt(4f) peaks compared to those of Au.

Errors, which can arise from not using the appropriate asymmetric line shapes, are illustrated in Fig. 6, which shows the overlapping Au(4d)-Pd(3d) region for nanoparticles of metallic Au and Pd together with the presence of Pd^{2+} supported on TS-1, a catalyst commonly used for the *in situ* generation of hydrogen peroxide for oxidation reactions in academic research laboratories.[70–72]

In Fig. 6(a), the spectrum has been fitted using a simple Gaussian–Lorentzian function for all peak shapes. While reflecting the presence of both Pd and Au and their relative spin–orbit splitting and area ratios, the fitting has two significant issues: First, the FWHM of the Pd(3d) peaks is significantly broader (~3 eV) than expected, given the system resolution and operating conditions. Second, in an attempt to match the data envelope, a second Pd species has been included, exhibiting an unrealistically high Pd ($3d_{5/2}$) binding energy of 340.8 eV, significantly higher than any known Pd chemical state.[50]

Contrastingly, Fig. 6(b) is fitted with a single state for Au and two states of Pd (metallic and PdO) using line shapes derived from standard materials. Not only does this yield a fit more in line with the spectral envelope but, more importantly, one which reflects the catalyst structure and activity. Additionally, a comparison of the Au(4d) derived atomic concentration with that of the Au(4f) derived atomic concentrations gives a confidence limit of ±0.1 at. %. The advantage of such a methodology is that it allows the derivation of peak shapes and constraints such as spin–orbit splitting, FWHM, and peak area relationships so that models can be readily transferred between data sets and reducing uncertainty in peak fits by minimizing the number of parameters required to fit. The spectrum in Fig. 6(b), for example, was allowed a small movement in the position of the Au and Pd peaks (~0.5 eV) from their bulk values and relaxation of the most intense peak FWHM to allow for the difference in charging, for example.

Such asymmetry is not only evident in metals. Graphitic carbon and conducting oxides, such as RuO_2 and IrO_2, also exhibit asymmetric core levels, with the oxides also exhibiting asymmetric O(1s) core levels.[46,73–76] Furthermore, the spectral envelope can change depending on levels of hydration.[46,74] It is strongly recommended, therefore, to do a thorough search of the literature and whenever possible, for the analyst to measure their own fresh, high-purity, and well characterized standard materials as a point of reference to create their own material database.

B. Chemical state identification and Auger lines

Chemical state identification is typically made from binding energy assignments of spectra calibrated to a suitable reference (see Sec. IV). However, binding energies can be misleading; they may, for example, be affected by particle size;[39,77–82] or the core levels may not significantly shift between chemical states (e.g., Zn versus ZnO). In such cases, the analyst may use other core levels that they have identified and recorded during their experimental design; for example, the magnitude of the splitting observed for the Mn(3s) peak has often been used to elucidate the Mn oxidation state,[83–86] although recent studies have suggested that care should be taken with such approaches.[87]

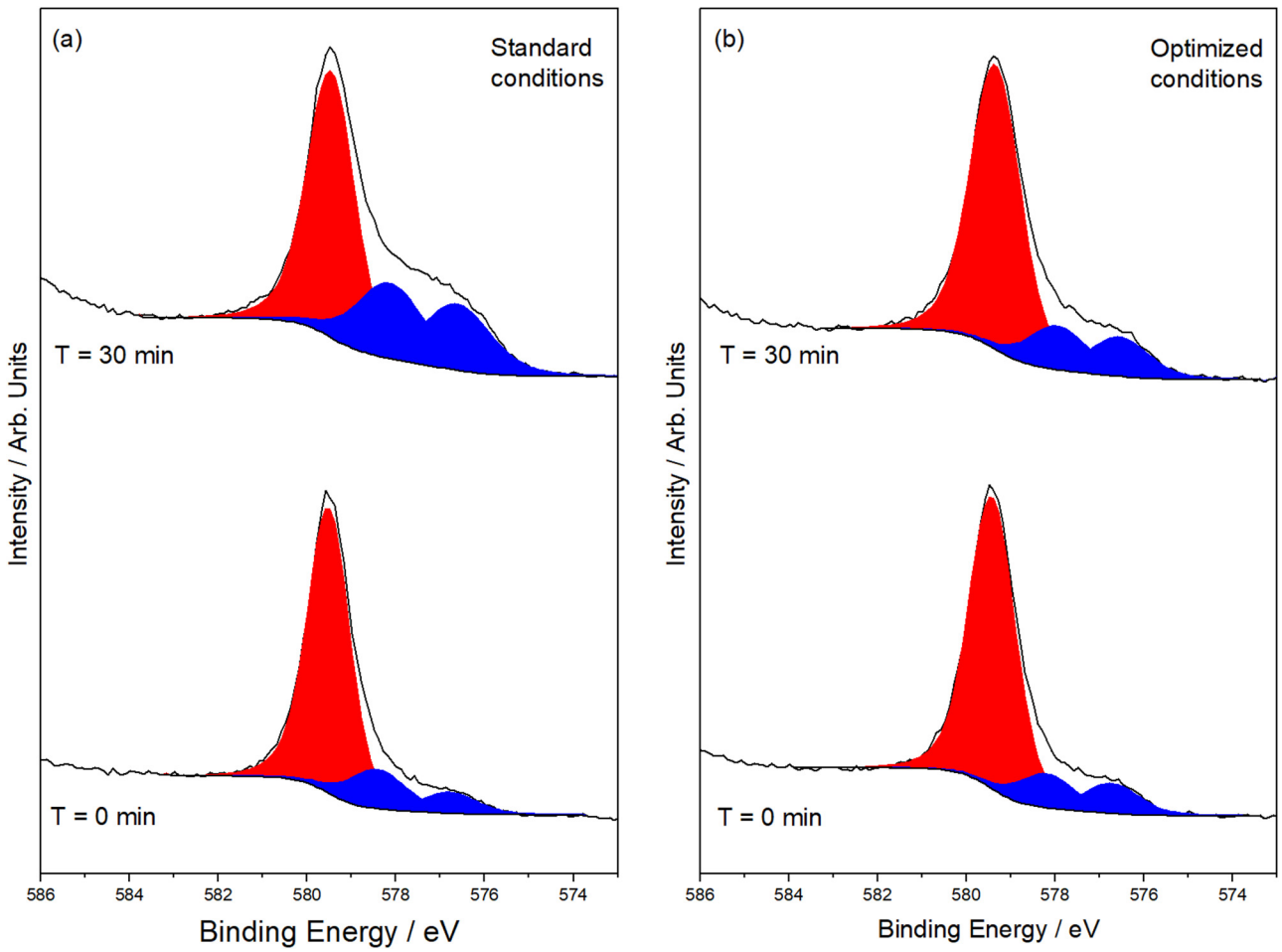

FIG. 3. $Cr(2p_{3/2})$ core-level spectra for CrO_3 flakes taken at before (T = 0 min) and after 30 min analysis, where spectra in (a) are recorded using the default neutralizer conditions and (b) are recorded using optimized charge compensation source parameters, which minimizes the reduction rate. Note that although some initial Cr^{3+} reduced states are present (colored blue online, fitted as Cr_2O_3 at lower binding energies), the concentrations of these do not influence the observed reduction.

Greater confidence can be found in using the x-ray induced Auger lines to aid chemical state identification as described by Wagner[88] and utilizing Auger parameters and chemical state plots (commonly called Wagner plots).[89,90] The usefulness of such analysis in chemical state identification is widely reported and exemplified by the work of Moretti and co-workers.[91–94]

The differential of the C(KLL) Auger signal has found use in the analysis of carbon materials;[95,96] however, surface contamination and the difference in information depth of C(1s) and KLL Auger lines will increase uncertainty in the sp^2/sp^3 ratio.[96,97] More recently, Auger lines are being used more quantitatively;[98] however, while powerful, such analysis is not always possible in practice for catalytic systems, where prolonged acquisition times are required when the active component is frequently present at very low loadings, which can potentially lead to sample modification (see Sec. III).

Metal oxides may exhibit a complex O(1s) envelope, which can be comprised of lattice oxygen, hydroxyl, carbonate, and organic species and thus complicating the analysis of absolute Auger and core-level photoelectron energies. However, an insight into the oxide's surface electronic properties can be elucidated from the O (KLL) Auger lines and the associated Auger parameter (α), where α = kinetic energy (Auger line) + binding energy (photoemission line) since the emission is from a common core level. Relative to gaseous water [α = 1038.5 eV (Ref. 99], increasing values of α with decreasing separation of the O $KL_{23}L_{23}$ and O KL_1L_{23} signals indicate increasing surface polarizability and hence facilitates a quantitative measurement of Lewis basicity.[99–103]

C. Fresh, *in situ*, and postmortem analysis of samples

The majority of data presented at conferences or within peer reviewed journals primarily focuses on the "fresh" state of a catalyst, yielding valuable information on the initial chemical states on the surface. However, *in situ* treatments, "pseudo *in situ*" (where the

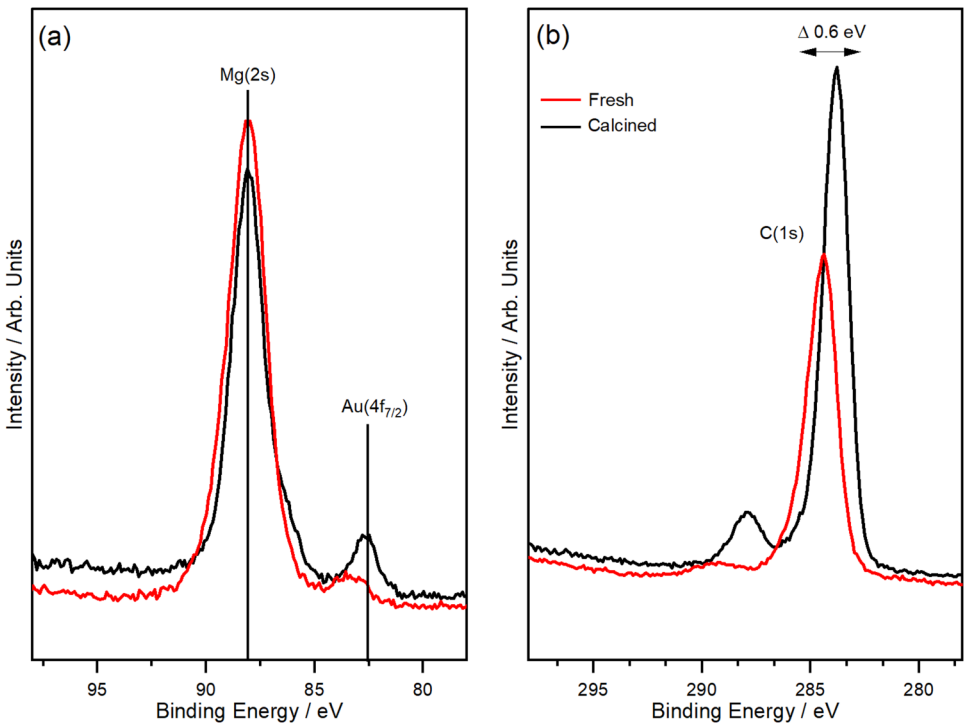

FIG. 4. Fresh (red color online) and calcined (black color online) overlay of (a) Mg(2s)/Au(4f) and (b) C(1s) core-level spectra for a 1% Au/MgO catalyst, indicating the caution of taking a specified peak as a constant value.

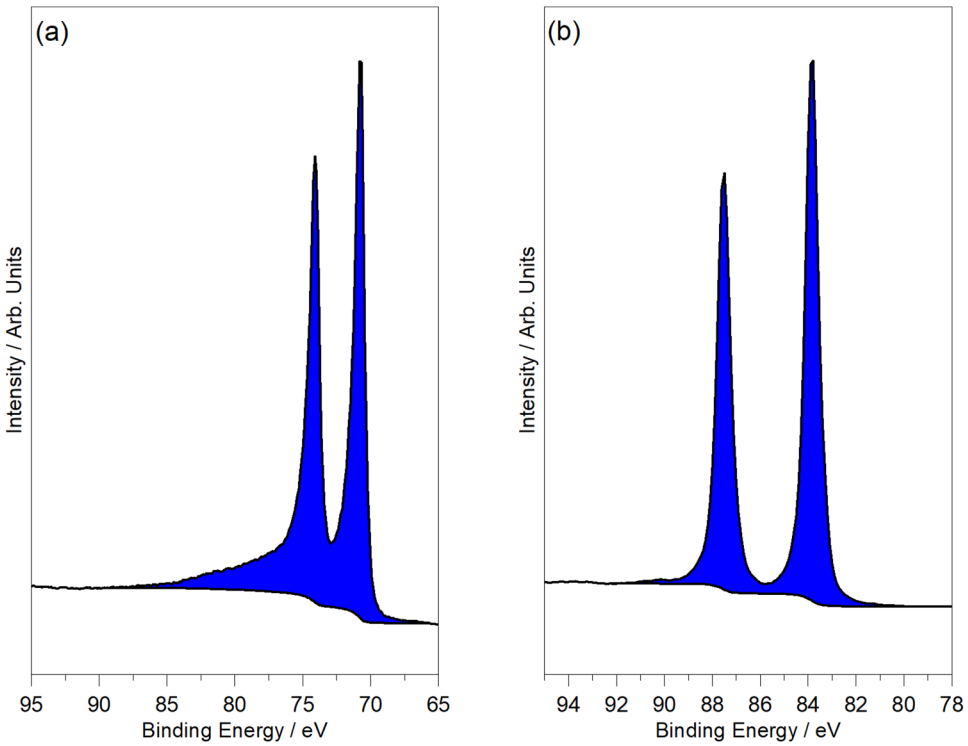

FIG. 5. (a) Pt(4f) and (b) Au(4f) core-level spectra of the neighboring metals, colored to highlight the increased asymmetry for Pt over Au.

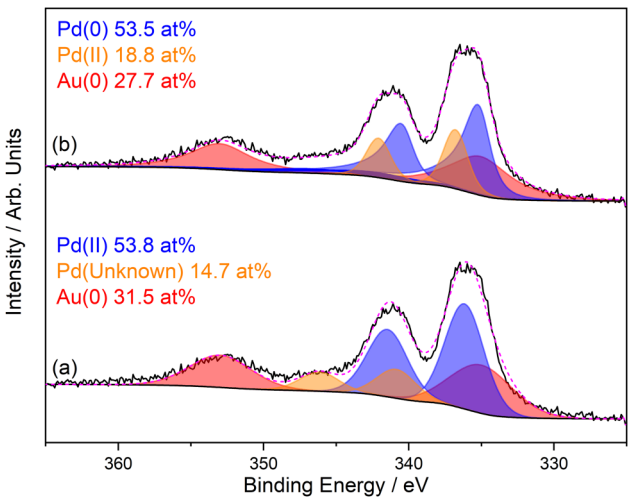

FIG. 6. Pd(3d)/Au(4d) spectra of an AuPd/TS-1 catalyst, where (a) data have been incorrectly fitted using simple Gaussian–Lorentzian functions and (b) the corrected fitting based on line shapes derived from models.

sample is removed from the catalytic reactor at different intervals for analysis), and postmortem analysis of catalysts can yield significant insights into the active species or deactivation of a catalyst, be it through formation of a particular chemical state,[11,104] leaching,[105,106] sintering,[107,108] formation of strongly bound species,[8,109] or coke formation.[110,111]

To exemplify this, we briefly compare the fresh and postmortem analysis of a $Fe_xCr_yO_z$ catalyst used for propane dehydrogenation (Fig. 7).

For the fresh catalyst, it is evident from Fig. 7(c) that both Cr^{6+} and Cr^{3+} species are present, whereas the used catalyst possesses only Cr^{3+} [Fig. 7(f)]; note here the high kinetic energy (low binding energy) peaks have been recorded in addition to the standard core levels [e.g., Cr(2p) and Fe(2p)] since the escape depth of these photoelectrons will be similar and less affected by the attenuating carbon overlayer. For some materials, such as uranium, analysis of these high kinetic energy lines proves more beneficial in the determination of the oxidation state than the main core-lines.[112]

Moreover, for the fresh catalyst, the carbon is adventitious and only 3% of the total elemental concentration, whereas for the spent catalyst, carbon accounts for over 80% of the total concentration and, as shown in Fig. 7(e), exhibits a shape typical of graphitic carbon[97] and indicating severe coking during the reaction. From Figs. 7(a) and 7(d), the relative amounts of Cr, Fe, and Na have also changed, potentially indicating sintering.

Understanding that coking is occurring in such catalysts is important as it allows tuning of the Cr/Fe content and chemical states to influence selectivity to propene formation and limit the rate of coke formation.[113] With the analysis of the XAES D-parameter[95,96] or via the advent of coincident Raman spectroscopy on XPS systems, further insights into the aromaticity of the coke may be examined.[114,115]

D. Determination of particle size and dispersion

One of the biggest factors in the activity of catalysis is particle size, which in turn affects dispersion. While x-ray diffraction or chemisorption methods are used for particle size determination, both techniques have limitations; the former relies on long-range order to obtain crystals of sufficient size for Bragg diffraction (~5 nm), whereas in the latter, geometric factors of the particles are typically ignored. The surface sensitivity of XPS means that it is ideally suited to recognizing how well particles are dispersed over a support material. If one assumes the case of two catalysts with an identical amount of material in the supported phase, then for a case where very small particles are present, the surface is to a large extent covered by the nanoparticles. For where the particles are larger, however, the dispersion is poor, and hence if we ratio the photoelectron signal from the particle (Ip) to that of the support (Is), then we have a case where Ip/Is is low for poorly dispersed particles and high for well dispersed particles.

Extending this, Kerkhof and Moulijn[32] proposed a simple model (later simplified by León[116]) for the determination of particle sizes, which uses the aforementioned ratio for a quantitative estimation of the dispersion by modeling a supported catalyst as a stack of sheets with cuboid crystals representing support particles and has been shown to give excellent agreement with sizes derived from chemisorption measurements. A second method, relying on the intensity ratio for two core levels of significantly different kinetic energies, was proposed by Davis[117] and is independent of the catalyst surface area and loading. This method, which is especially suited to systems with monochromatic Ag sources for accessing higher binding energy photoemission lines, has been successfully applied to a number of systems,[117–120] provided that the particles sizes are below ~2λ (where λ is the electron inelastic mean free path), although contamination overlayers, which would attenuate lower kinetic energy signals, would limit accuracy; however, such an analysis requirement would feed into the experimental planning stage.

Other methods to extract particle size information include well-defined changes in binding energy and analysis of energy-loss electrons within the photoelectron background.[80,121] Such particle size information from XPS has allowed correlation with the catalytic turnover frequency.[122–124]

Many supported particles may be of a core-shell, or similar, morphology, and will, therefore, have photoelectron intensity ratios influenced by the core-shell morphology. Shard has developed models to account for such morphologies and but accuracy may be there is a significant difference in the kinetic energies of the core and shell materials are widely different.[125] Such spectra may also be modeled through the use of simulation software, such as SESSA,[126] to evaluate the inner structure of core-shell morphologies.[127,128]

For all the models in this section, the theory and mathematics of each method are beyond the scope of this paper, and readers are encouraged to review the relevant supplied references.

E. High energy XPS (HAXPES) in catalysis

While higher energy sources have been available for many years,[129–133] their wider use has been somewhat precluded by primarily wide-scale availability, broader linewidths, and decreased

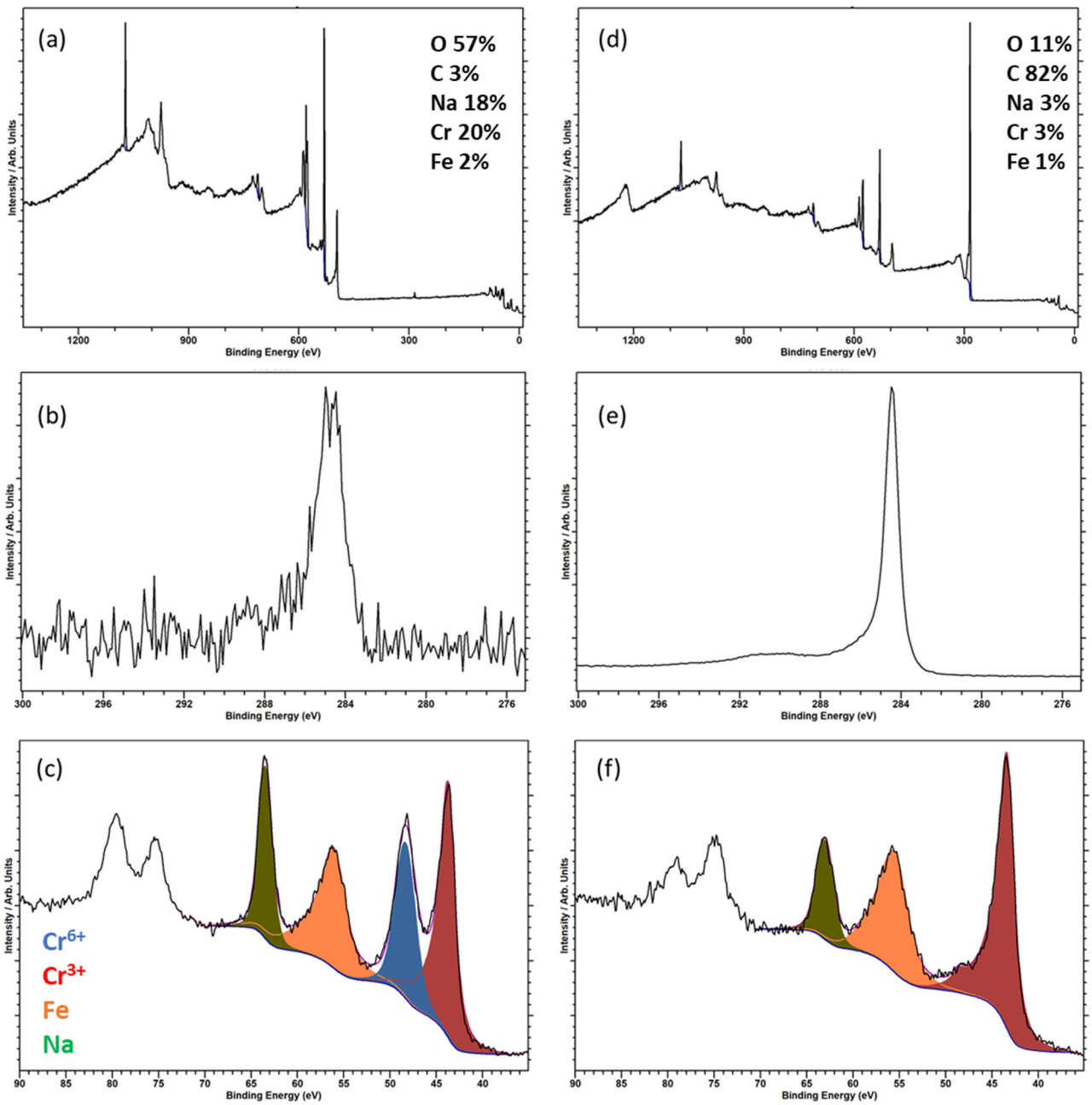

FIG. 7. Survey, C(1s), and Cr(3p)/Fe(3p)/Na(2s) core-level spectra for (a)–(c) fresh catalyst and (d)–(f) used catalyst, respectively.

elemental sensitivity to orbitals conventionally studied with Al/Mg radiation.[134] Many instrument manufacturers now routinely offer monochromatic Ag or Cr sources, and their use is still somewhat in their infancy in catalysis for lab-based systems, with many studies still reliant on synchrotron radiation.[135,136]

Despite the lower sensitivity to many orbitals routinely analyzed using Al/Mg excitation for higher photon energy sources, the depth information, which may be obtained by relatively simple measurements, can greatly enhance information, for example, zeolites and 2D materials, or facilitate extraction of layer information via Tougaard analysis.[137–139]

Of course, the question "why use such lab-based HAXPES sources in the analysis of catalytic materials since catalysis is a surface phenomenon" can be raised. We have already highlighted

the use in particle size determination (Sec. V D); however, it should be noted that both subsurface and bulk compositions can influence surface properties; therefore, being able to gauge such information is useful. Additionally, using such sources on coked material, such as those shown in Fig. 7, can facilitate the analysis of the buried interfacial chemistry.

VI. CONCLUSIVE SUMMARY

XPS is a lynchpin in the analysis of catalytic materials allowing quantitative chemical speciation and the ability to probe the electronic structure and the morphological character of a material. It has the power to differentiate chemical states, obtain molar ratios, and elucidate catalytic dispersion and particle size when results from other techniques may be obtuse.

Without considered planning, however, XPS measurements can yield misleading results due to poorly informed analysis protocols or data misinterpretation. It is evident that the information obtained from each analysis will be different since the questions to be answered for each sample will vary. The definition of the questions to be answered by means of the analysis beforehand help achieve an informed analysis protocol for each sample, which we hope have been brought to attention within this paper.

ACKNOWLEDGMENTS

The authors wish to express their sincere thanks to all their mentors, colleagues, and co-workers who, over many years, have facilitated the great science to which the authors have been part of. Some of the work included herein has been generated through the authors' provision of the EPSRC National Facility for Photoelectron Spectroscopy (HarwellXPS), operated by Cardiff University and UCL under Contract No. PR16195.

REFERENCES

[1]M. S. Spencer, "Fundamental principles," in *Catalyst Handbook*, edited by M. V. Twigg (CRC, Boca Raton, FL, 1989).
[2]B. C. Gates, *Catalytic Chemistry* (Wiley, Chichester, 1992).
[3]J. Hagen, *Industrial Catalysis: A Practical Approach* (Wiley-VCH, Weinheim, 2015).
[4]A. M. Venezia, Catal. Today **77**, 359 (2003).
[5]J. F. Watts and J. Wolstenholme, *An Introduction to Surface Analysis by XPS and AES*, 2nd ed. (Wiley, Chichester, 2003).
[6]J. H. Carter, P. M. Shah, E. Nowicka, S. J. Freakley, D. J. Morgan, S. Golunski, and G. J. Hutchings, Front. Chem. **7**, 443 (2019).
[7]G. W. Coulston, E. A. Thompson, and N. Herron, J. Catal. **163**, 122 (1996).
[8]D. R. Jones, S. Iqbal, P. J. Miedziak, D. J. Morgan, J. K. Edwards, Q. He, and G. J. Hutchings, Top. Catal. **61**, 833 (2018).
[9]E. Nowicka *et al.*, Catal. Sci. Technol. **8**, 5848 (2018).
[10]T. M. Nyathi, N. Fischer, A. P. E. York, D. J. Morgan, G. J. Hutchings, E. K. Gibson, P. P. Wells, C. R. A. Catlow, and M. Claeys, ACS Catal. **9**, 7166 (2019).
[11]X. Liu, M. Conte, D. Elias, L. Lu, D. J. Morgan, S. J. Freakley, P. Johnston, C. J. Kiely, and G. J. Hutchings, Catal. Sci. Technol. **6**, 5144 (2016).
[12]G. Malta *et al.*, Science **355**, 1399 (2017).
[13]M. Schindler, F. C. Hawthorne, M. S. Freund, and P. C. Burns, Geochim. Cosmochim. Acta **73**, 2471 (2009).
[14]D. J. Tobler, J. D. Rodriguez-Blanco, K. Dideriksen, N. Bovet, K. K. Sand, and S. L. S. Stipp, Adv. Funct. Mater. **25**, 3081 (2015).
[15]D. R. Baer *et al.*, J. Vac. Sci. Technol. A **37**, 031401 (2019).
[16]I. A. Leenson, J. Chem. Educ. **82**, 241 (2005).
[17]Y. Mikhlin, A. Karacharov, Y. Tomashevich, and A. Shchukarev, J. Electron Spectrosc. Relat. Phenom. **206**, 65 (2016).
[18]N. Tsud, V. Johánek, I. Stará, K. Veltruská, and V. Matolín, Thin Solid Films **391**, 204 (2001).
[19]X. Chen *et al.*, Sci. Rep. **3**, 1510 (2013).
[20]G. Beamson and D. Briggs, *High Resolution XPS of Organic Polymers: The Scienta ESCA300 Database* (Wiley, Chichester, 1992).
[21]M. Engelhard, D. Baer, and S. Lea, Surf. Sci. Spectra **10**, 80 (2003).
[22]Y. Y. Fong, B. R. Visser, J. R. Gascooke, B. C. Cowie, L. Thomsen, G. F. Metha, M. A. Buntine, and H. H. Harris, Langmuir **27**, 8099 (2011).
[23]M. Conte, C. J. Davies, D. J. Morgan, A. F. Carley, P. Johnston, and G. J. Hutchings, Catal. Lett. **144**, 1 (2013).
[24]T. H. Fleisch and G. J. Mains, J. Phys. Chem. **90**, 5317 (1986).
[25]S. Iqbal, M. L. Shozi, and D. J. Morgan, Surf. Interface Anal. **49**, 223 (2017).
[26]M. C. Biesinger, L. W. M. Lau, A. R. Gerson, and R. S. C. Smart, Appl. Surf. Sci. **257**, 887 (2010).
[27]Ş Süzer, Appl. Spectrosc. **54**, 1716 (2016).
[28]D. Baer, M. Engelhard, D. Gaspar, and S. Lea, "Beam effects during AES and XPS analysis," in *Surface Analysis by Auger and X-ray Photoelectron Spectroscopy*, edited by D. Briggs and J. T. Grant (IM Publications, Chichester, 2003).
[29]J. H. Thomas III, "Photon beam damage and charging at solid surfaces," in *Beam Effects, Surface Topography and Depth Profiling in Surface Analysis*, edited by A. W. Czanderna, T. E. Madey, and C. J. Powell (Plenum, New York, 1998), p. 1.
[30]L. Edwards, P. Mack, and D. J. Morgan, Surf. Interface Anal. **51**, 925 (2019).
[31]V. Di Castro, C. Furlani, M. Gargano, N. Ravasio, and M. Rossi, J. Electron Spectrosc. Relat. Phenom. **52**, 415 (1990).
[32]F. P. J. M. Kerkhof and J. A. Moulijn, J. Phys. Chem. **83**, 1612 (1979).
[33]J. W. Niemantsverdriet, *Spectroscopy in Catalysis*, 3rd ed. (Wiley-VCH, Weinheim, 2007).
[34]C. J. Powell, "Calibrations and checks of the binding-energy scales of X-ray photoelectron spectrometers," J. Electron Spectrosc. Relat. Phenom. (in press).
[35]A. Fernández, A. Caballero, and A. R. González-Elipe, Surf. Interface Anal. **18**, 392 (1992).
[36]A. Frydman, D. G. Castner, M. Schmal, and C. T. Campbell, J. Catal. **152**, 164 (1995).
[37]N. Kruse and S. Chenakin, Appl. Catal. A **391**, 367 (2011).
[38]A. Lewera, L. Timperman, A. Roguska, and N. Alonso-Vante, J. Phys. Chem. C **115**, 20153 (2011).
[39]K. Luo, D. Y. Kim, and D. W. Goodman, J. Mol. Catal. A Chem. **167**, 191 (2001).
[40]R. Radnik, C. Mohr, and P. Claus, Phys. Chem. Chem. Phys. **5**, 172 (2003).
[41]B. V. Crist, J. Electron Spectrosc. Relat. Phenom. **231**, 75 (2019).
[42]R. Blume, D. Rosenthal, J.-P. Tessonnier, H. Li, A. Knop-Gericke, and R. Schlögl, Chem. Cat. Chem. **7**, 2871 (2015).
[43]O. Böse, E. Kemnitz, A. Lippitz, and W. E. S. Unger, Fresenius J. Anal. Chem. **358**, 175 (1997).
[44]S. Kohiki and K. Oki, J. Electron Spectrosc. Relat. Phenom. **33**, 375 (1984).
[45]W. E. S. Unger, T. Gross, O. Bose, U. Gelius, T. Fritz, and A. Lippitz, Surf. Interface Anal. **29**, 535 (2000).
[46]D. J. Morgan, Surf. Interface Anal. **47**, 1072 (2015).
[47]M. Jacquemin, M. J. Genet, E. M. Gaigneaux, and D. P. Debecker, Chem. Phys. Chem. **14**, 3618 (2013).
[48]G. Greczynski and L. Hultman, Chem. Phys. Chem. **18**, 1507 (2017).
[49]G. Greczynski and L. Hultman, Appl. Surf. Sci. **451**, 99 (2018).
[50]*NIST X-ray Photoelectron Spectroscopy Database*, Version 4.1, National Institute of Standards and Technology, Gaithersburg, 2012, see http://srdata.nist.gov/xps/.
[51]A. K. Bhattacharya, D. R. Pyke, R. Reynolds, G. S. Walker, and A. K. Bhattacharya, J. Mater. Sci. Lett. **16**, 1 (1997).

[52]M. J. Remy, M. J. Genet, G. Poncelet, P. F. Lardinois, and P. P. Notte, J. Phys. Chem. **96**, 2614 (1992).
[53]E. Paparazzo, G. M. Ingo, and N. Zacchetti, J. Vac. Sci. Technol. A **9**, 1416 (1991).
[54]M. M. Natile and A. Glisenti, Surf. Sci. Spectra **13**, 17 (2006).
[55]C. Barth, C. Laffon, R. Olbrich, A. Ranguis, P. Parent, and M. Reichling, Sci. Rep. **6**, 21165 (2016).
[56]D.-G. Cheng, M. Chong, F. Chen, and X. Zhan, Catal. Lett. **120**, 82 (2007).
[57]*Surface Science Spectra*, see http://avs.scitation.org/journal/sss
[58]Y. A. Teterin and A. Y. Teterin, Russ. Chem. Rev. **71**, 347 (2002).
[59]J. Balcerzak, W. Redzynia, and J. Tyczkowski, Appl. Surf. Sci. **426**, 852 (2017).
[60]B. Desalegn, M. Megharaj, Z. Chen, and R. Naidu, Heliyon **5**, e01750 (2019).
[61]J. H. Kim, J. Y. Cheon, T. J. Shin, J. Y. Park, and S. H. Joo, Carbon **101**, 449 (2016).
[62]K. W. Brinkley, M. Burkholder, A. R. Siamaki, K. Belecki, and B. F. Gupton, Green Process. Synth. **4**, 241 (2015).
[63]I. Roger, R. Moca, H. N. Miras, K. G. Crawford, D. A. J. Moran, A. Y. Ganin, and M. D. Symes, J. Mater. Chem. A **5**, 1472 (2017).
[64]A. M. García *et al.*, J. Mater. Chem. A **6**, 1119 (2018).
[65]M. Zannotti, C. J. Wood, G. H. Summers, L. A. Stevens, M. R. Hall, C. E. Snape, R. Giovannetti, and E. A. Gibson, ACS Appl. Mater. Interfaces **7**, 24556 (2015).
[66]N. Poldme *et al.*, Chem. Sci. **10**, 99 (2019).
[67]P. M. A. Sherwood, Surf. Interface Anal. **51**, 589 (2019).
[68]D. Briggs, "XPS basic principles, spectral features and qualitative analysis," in *Surface Analysis by Auger and X-ray Photoelectron Spectroscopy*, edited by D. Briggs and J. T. Grant (IM Publications, Chichester, 2003).
[69]H. Höchst, S. Hüfner, and A. Goldmann, Phys. Lett. A **57**, 265 (1976).
[70]R. J. Lewis *et al.*, Chem. Cat. Chem. **11**, 1673 (2019).
[71]V. R. Choudhary, N. S. Patil, and S. K. Bhargava, Catal. Lett. **89**, 55 (2003).
[72]D. J. Robinson *et al.*, Phys. Chem. Chem. Phys. **2**, 1523 (2000).
[73]P. A. Cox, J. B. Goodenough, P. J. Tavener, D. Telles, and R. G. Egdell, J. Solid State Chem. **62**, 360 (1986).
[74]S. J. Freakley, J. Ruiz-Esquius, and D. J. Morgan, Surf. Interface Anal. **49**, 794 (2017).
[75]Y. J. Kim, Y. Gao, and S. A. Chambers, Appl. Surf. Sci. **120**, 250 (1997).
[76]G. K. Wertheim and H. J. Guggenheim, Phys. Rev. B **22**, 4680 (1980).
[77]I. Aruna, B. R. Mehta, L. K. Malhotra, and S. M. Shivaprasad, J. Appl. Phys. **104**, 064308 (2008).
[78]B. Balamurugan and T. Maruyama, Appl. Phys. Lett. **89**, 033112 (2006).
[79]A. F. Carley, L. A. Dollard, P. R. Norman, C. Pottage, and M. W. Roberts, J. Electron Spectrosc. Relat. Phenom. **98**, 223 (1999).
[80]A. R. Gonzalez-Elipe, G. Munuera, and J. P. Espinos, Surf. Interface Anal. **16**, 375 (1990).
[81]G. Lassaletta, A. Fernandez, J. P. Espinos, and A. R. Gonzalez-Elipe, J. Phys. Chem. **99**, 1484 (1995).
[82]J. Morales, A. Caballero, J. P. Holgado, J. P. Espinós, and A. R. González-Elipe, J. Phys. Chem. B **106**, 10185 (2002).
[83]J. L. Junta and M. F. Hochella, Geochim. Cosmochim. Acta **58**, 4985 (1994).
[84]D. Banerjee and H. W. Nesbitt, Geochim. Cosmochim. Acta **63**, 3025 (1999).
[85]D. Banerjee and H. W. Nesbitt, Geochim. Cosmochim. Acta **63**, 1671 (1999).
[86]D. Banerjee and H. W. Nesbitt, Geochim. Cosmochim. Acta **65**, 1703 (2001).
[87]E. S. Ilton, J. E. Post, P. J. Heaney, F. T. Ling, and S. N. Kerisit, Appl. Surf. Sci. **366**, 475 (2016).
[88]C. D. Wagner, Anal. Chem. **44**, 967 (2002).
[89]C. D. Wagner, L. H. Gale, and R. H. Raymond, Anal. Chem. **51**, 466 (2002).
[90]C. D. Wagner, Faraday Discuss. Chem. Soc. **60**, 496 (1975).
[91]G. Moretti, F. Filippone, and M. Satta, Surf. Interface Anal. **31**, 249 (2001).
[92]G. Moretti, J. Electron Spectrosc. Relat. Phenom. **95**, 95 (1998).
[93]G. Moretti, Surf. Sci. **618**, 3 (2013).
[94]G. Moretti, A. Palma, E. Paparazzo, and M. Satta, Surf. Sci. **646**, 298 (2016).
[95]J. C. Lascovich and S. Scaglione, Appl. Surf. Sci. **78**, 17 (1994).
[96]B. Lesiak, L. Kövér, J. Tóth, J. Zemek, P. Jiricek, A. Kromka, and N. Rangam, Appl. Surf. Sci. **452**, 223 (2018).
[97]D. J. Morgan, Surf. Sci. Spectra **24**, 024003 (2017).
[98]M. C. Biesinger, Surf. Interface Anal. **49**, 1325 (2017).
[99]J. A. D. Matthew and S. Parker, J. Electron Spectrosc. Relat. Phenom. **85**, 175 (1997).
[100]J. M. Montero, P. Gai, K. Wilson, and A. F. Lee, Green Chem. **11**, 265 (2009).
[101]G. Moretti, J. Electron Spectrosc. Relat. Phenom. **58**, 105 (1992).
[102]P. Ascarelli and G. Moretti, Surf. Interface Anal. **7**, 8 (1985).
[103]J. van den Brand, P. C. Snijders, W. G. Sloof, H. Terryn, and J. H. W. de Wit, J. Phys. Chem. B **108**, 6017 (2004).
[104]G. Malta, S. J. Freakley, S. A. Kondrat, and G. J. Hutchings, Chem. Commun. **53**, 11733 (2017).
[105]Y. Ji, S. Jain, and R. J. Davis, J. Phys. Chem. B **109**, 17232 (2005).
[106]A. A. Youzbashi and S. G. Dixit, Metall. Mater. Trans. B **22**, 775 (1991).
[107]S. Wodiunig, J. M. Keel, T. S. E. Wilson, F. W. Zemichael, and R. M. Lambert, Catal. Lett. **87**, 1 (2003).
[108]Y. Niu, P. Schlexer, B. Sebok, I. Chorkendorff, G. Pacchioni, and R. E. Palmer, Nanoscale **10**, 2363 (2018).
[109]S. Iqbal *et al.*, ACS Catal. **5**, 5047 (2015).
[110]B. Sexton, J. Catal. **109**, 126 (1988).
[111]B. S. Liu, L. Jiang, H. Sun, and C. T. Au, Appl. Surf. Sci. **253**, 5092 (2007).
[112]E. S. Ilton, Y. Du, J. E. Stubbs, P. J. Eng, A. M. Chaka, J. R. Bargar, C. J. Nelin, and P. S. Bagus, Phys. Chem. Chem. Phys. **19**, 30473 (2017).
[113]O. F. Gorriz, V. Cortes Corberan, and J. L. G. Fierro, Ind. Eng. Chem. Res. **31**, 2670 (1992).
[114]P. C. Stair, Adv. Catal. **51**, 75 (2007).
[115]S. R. Bare *et al.*, ACS Catal. **7**, 1452 (2017).
[116]V. León, Surf. Sci. **339**, L931 (1995).
[117]S. M. Davis, J. Catal. **117**, 432 (1989).
[118]R. Wojcieszak, A. Karelovic, E. M. Gaigneaux, and P. Ruiz, Catal. Sci. Technol. **4**, 3298 (2014).
[119]M. Y. Smirnov, A. V. Kalinkin, A. V. Bukhtiyarov, I. P. Prosvirin, and V. I. Bukhtiyarov, J. Phys. Chem. C **120**, 10419 (2016).
[120]M. N. Ghazzal, R. Wojcieszak, G. Raj, and E. M. Gaigneaux, Beilstein J. Nanotechnol. **5**, 68 (2014).
[121]S. Hajati, V. Zaporojtchenko, F. Faupel, and S. Tougaard, Surf. Sci. **601**, 3261 (2007).
[122]L. V. Nosova, M. V. Stenin, Y. N. Nogin, and Y. A. Ryndin, Appl. Surf. Sci. **55**, 43 (1992).
[123]A. M. Venezia, A. Rossi, D. Duca, A. Martorana, and G. Deganello, Appl. Catal. A **125**, 113 (1995).
[124]G. Deganello, D. Duca, A. Martorana, G. Fagherazzi, and A. Benedetti, J. Catal. **150**, 127 (1994).
[125]A. G. Shard, J. Phys. Chem. C **116**, 16806 (2012).
[126]W. Smekal, W. S. M. Werner, and C. J. Powell, Surf. Interface Anal. **37**, 1059 (2005).
[127]M. Chudzicki, W. S. Werner, A. G. Shard, Y. C. Wang, D. G. Castner, and C. J. Powell, J. Phys. Chem. C **119**, 17687 (2015).
[128]M. Chudzicki, W. S. M. Werner, A. G. Shard, Y. C. Wang, D. G. Castner, and C. J. Powell, J. Phys. Chem. C **120**, 2484 (2016).
[129]M. J. Edgell, R. W. Paynter, and J. E. Castle, J. Electron Spectrosc. Relat. Phenom. **37**, 241 (1985).
[130]J. E. Castle, L. B. Hazell, and R. D. Whitehead, J. Electron Spectrosc. Relat. Phenom. **9**, 247 (1976).
[131]C. D. Wagner, J. Vac. Sci. Technol. **15**, 518 (1978).
[132]J. E. Castle and R. H. West, J. Electron Spectrosc. Relat. Phenom. **19**, 409 (1980).
[133]S. Diplas, J. F. Watts, S. A. Morton, G. Beamson, P. Tsakiropoulos, D. T. Clark, and J. E. Castle, J. Electron Spectrosc. Relat. Phenom. **113**, 153 (2001).

[134]A. G. Shard, J. D. P. Counsell, D. J. H. Cant, E. F. Smith, P. Navabpour, X. Zhang, and C. J. Blomfield, Surf. Interface Anal. **51**, 763 (2019).
[135]S. R. Bare *et al.*, Surf. Sci. **648**, 376 (2016).
[136]C. Song *et al.*, Nanoscale Adv. **1**, 546 (2019).
[137]S. Tougaard, J. Surf. Anal. **24**, 107 (2017).
[138]C. Zborowski and S. Tougaard, Surf. Interface Anal. **51**, 857 (2019).
[139]P. Risterucci, O. Renault, E. Martinez, B. Detlefs, J. Zegenhagen, G. Grenet, and S. Tougaard, Surf. Interface Anal. **46**, 906 (2014).